Accepted Manuscript

Response of Aluminium Honeycomb Sandwich Panels Subjected to Foam Projectile Impact – An Experimental Study

M.A. Yahaya, D. Ruan, G. Lu, M.S. Dargusch

Please cite this article as: Yahaya MA, Ruan D, Lu G, Dargusch MS, Response of Aluminium Honeycomb Sandwich Panels Subjected to Foam Projectile Impact – An Experimental Study, *International Journal of Impact Engineering* (2014), doi: 10.1016/j.ijimpeng.2014.07.019.

Response of Aluminium Honeycomb Sandwich Panels Subjected to Foam Projectile Impact – An Experimental Study

M. A. Yahaya[a,b], D. Ruan[a,*], G. Lu[c], M.S Dargusch[d]

[a]Defence Materials Technology Centre, Faculty of Science, Engineering and Technology, Swinburne University of Technology Hawthorn, VIC 3122, Australia

[b]Faculty of Mechanical Engineering, Universiti Teknologi MARA, Shah Alam, 40450, Malaysia

[c]School of Mechanical and Aerospace Engineering, Nanyang Technological University, Singapore 639798

[d]Defence Materials Technology Centre, School of Mechanical and Mining Engineering, The University of Queensland, St Lucia, QLD 4072, Australia

Abstract

Aluminium honeycomb sandwich panels have potential applications as a protective mechanism that can be used to prevent failure of an important structure subjected to impact loading. Therefore it is important to fully understand the resistance of the sandwich panels subjected to impact loading conditions. The main objective of this work was to study the resistance of sandwich panels with different aluminium honeycomb cores, air sandwich panels (no core between the two face sheets) and monolithic plates of equivalent mass subjected to impact from foam projectiles. The deformation and the elastic spring-back of the honeycomb sandwich panels and the monolithic plates have been compared and discussed. The resistance of the panels and plates has been quantified by their back-face deflection with respect to the projectile impulse. Five different types of aluminium honeycombs have been used as the core material. The front-face sheet and the back-face sheet of the honeycomb sandwich panels are made of aluminium plate with 1 mm thickness. Cylindrical ALPORAS

aluminium foams with a relative density between 9% and 11% are employed as the metal foam projectiles. They are fired at several hundred meters per second towards the centre of the panels and plates using a gas gun. The deflection histories of the back-face have been measured using a laser displacement sensor. From the deflection histories, the maximum deflection and the final deflection of the back-face can be distinguished. Deformation modes and failure modes of the individual component have been observed and classified into several categories. Moreover, the deflections of the honeycomb sandwich panels have been compared with deflections from air sandwich panels. It is found that the honeycomb sandwich panels outperform both the air sandwich panels and the monolithic plates within an impulse range of 2.25 kNsm^{-2} $\sim$ 4.70 kNsm^{-2}. Outside this operational range, the advantages associated with employing the honeycomb sandwich panels as a protective structure upon impact of foam projectiles diminishes.

*Corresponding author. Tel.: +61 3 9214 8258. E-mail address: <ins>druan@swin.edu.au</ins>

1. Introduction

There has been increasing interest in the design and development of impact resistance structures over the past decade. Sandwich panels with aluminium honeycomb cores have been identified as one of the potential candidate protective structures as they have a high strength to weight ratio and have a good energy absorption capacity [1]. However, their behaviour under impact loading remains to be fully understood. Radford et al. [2] developed an experimental technique to generate shock loading into a structure by using metal foam projectiles. More work has been carried out applying the method to study the dynamic

response and energy absorption capacity of honeycomb sandwich beams [3-8] and honeycomb sandwich panels [9-11] with different core configurations. Curve sandwich panels were also used to absorb shock loading [12]. Recently, metal foam projectiles have also been used to mimic the impact of a sand column against a structure [13].

The use of metal foam is becoming popular in the transportation industry such as in the construction of high speed vehicles in order to reduce weight and to save fuel consumption without compromising the safety standard. However, during a collision, fractured foam can fly off at velocities up to several hundred meters per second and hit the surrounding structures, similar to what happened to the Columbia Space Shuttle in 2003 where a piece of foam from the protective layer of the fuel tank struck the wing edge that was made of ultra-strong carbon composite panels [14, 15]. The accident took seven astronauts' lives. Such catastrophic failure could possibly be avoided if the data describing the threat of foam projectile impact had been available beforehand.

As a protective structure, the maximum deflection and the final deflection of the sandwich panels upon loading has to be clearly distinguished. The difference between the maximum deflection and the final deflection is known as elastic spring-back [16]. Using final deflection rather than maximum deflection as a design guideline has misled designers in optimising the capability of sandwich panels as a protective structure.

In this paper, ALPORAS aluminium foam projectiles have been used to impact the centre of aluminium honeycomb sandwich panels at several impact velocities by using a gas gun. Aluminium alloy plates have been used as the face sheets of the honeycomb sandwich panels. Previously, high strength stainless steel plates were used as the face sheets [3-8] and no

failure of the face sheets was reported. The current study has employed aluminium face sheets to investigate face sheet failure. Deformation of the sandwich panels has been studied by analysing the deformation and the failure modes of the face sheets and the core for different core configurations, while the resistance of the sandwich panels has been studied by measuring the back-face deflection of the panels. The back-face deflection of the sandwich panels has also been compared with monolithic plates of equivalent mass and air sandwich panels. The air sandwich panel has a structure which consists of only two parallel plates (without core) at a distance similar to the core thickness of honeycomb sandwich panels. Finally the back-face deflection histories of the sandwich panels have been compared with the deflection histories of monolithic plates of equivalent mass to determine the benefit of using sandwich panels in reducing elastic spring-back. The histories of the back-face deflection have been captured experimentally by using a laser displacement sensor. The advantages and limitations of using sandwich panels in absorbing impact energy of foam projectile impact have been discussed.

2. Experiments

2.1 Equipment

The experimental set-up is shown in Fig. 1. The set-up consists of a nitrogen gas tank, a pressure regulator, a gas gun, a velocity meter, a sample holder and a laser displacement sensor. The nitrogen gas tank supplies nitrogen gas to the gas gun at a pressure prescribed in the pressure regulator to propel the projectile. The gas gun has a barrel length of 3 m and an inner diameter of 38 mm. The sample holder is a special fixture fabricated to fully clamp the samples (include honeycomb sandwich panels, air sandwich panels and monolithic plates) at the end of the barrel. Due to the clamping along the samples, the exposed area of the samples has been reduced to 250 mm $\times$ 250 mm from their initial dimension of 300 mm $\times$ 300 mm.

There are a total of 16 M10 bolts on the clamp where 5 bolts are located at each side of the clamp, as shown in Fig.1. Extra caution was taken when fastening them manually to ensure not crushing the foam along edges, but enough to hold the sample firmly and uniformly along all edges. The velocity meter is installed in-between the barrel and the specimen holder in order to measure the velocity of foam projectiles just before impact. The laser displacement sensor has been manufactured by Micro-Epsilon Messtechnik Germany (Type LD 1607-200) and has been used to record the back-face deflection history of the sandwich panels. It is capable of measuring up to ±100 mm deformation from its reference distance which is located at 340 mm from the unit. The accuracy of the sensor is 0.01 mm. The laser spot, which is pointing at the centre of the back of the sandwich panel, has a diameter of 2 mm.

2.2 Specimens

2.2.1 Aluminium foam projectiles

The projectiles were made of aluminium foam with the brand name ALPORAS that had a composition of Al-Ca5-Ti3 (wt.%). The projectiles were cylindrical in shape with a length of $l_0 = 50$ mm and diameter of d = 37 mm. The preparation process of the projectiles included: cutting, drying and weighting. The projectiles were cut from a large block of aluminium foam using EDM. After the cutting process, the projectiles were left to dry for several days (water was used in the wire cutting process) and were weighed several times until the readings became consistent.

 The dimension and the mass of each projectile were then measured and the relative density was calculated accordingly before the tests. The relative density is defined as the ratio of the density of the foam to the density of aluminium, which is 2700 kgm^{-3}. Common cell morphological defects were observed on the foam projectiles such as misalignment and

broken cell wall, and non-uniform cell wall thickness and cell size. In order to minimize these defects, only projectiles with a relative density in the range of 9% to 11% were selected for the experiments. In this relative density range, the average cell size of the foam was 3 mm. A minimum ratio of the projectile size to the cell size of 5 is required in order to eliminate the size effect of cells [17]. Since the average cell size was 3 mm and the length and the diameters of the projectiles were 50 mm and 37 mm respectively, the ratio of the projectile size to the cell size was 16.7 along the length direction and 12.3 along the diameter direction.

2.2.2 *Aluminium honeycombs as the cores*

Five different types of HexWeb® hexagonal aluminium honeycombs were used as cores for the honeycomb sandwich panels. The honeycombs were manufactured by bonding together sheets of aluminium foil, then by expanding these sheets to form a cellular honeycomb configuration [18]. During the experiment, the aluminium honeycombs were varied in terms of honeycomb cell size and foil thickness. The cell size is defined as the distance between the two vertical walls of the hexagonal cell. The aluminium honeycombs are designated using Density – Cell Size – Foil Thickness and all dimensions are in imperial units. For example, 6.1-1/8-.0015 indicates an aluminium honeycomb with a density of 6.1 pcf (97.71 kgm^{-3}), cell size of 1/8 inches (3.18 mm) and foil thickness of .0015 inches (0.0381 mm). The height of all honeycombs is 0.5 inches which is equal to 12.7 mm. The properties of the honeycombs, which are provided by the manufacturer, are shown in Table 1.

2.2.3 *Aluminium face sheets*

The face sheets were made of aluminium alloy 5005 H34 with 1 mm thickness. Monolithic plates with thickness of 2 mm, 3 mm, 4 mm and 5 mm were tested as well for comparison. Quasi-static tensile tests at 0.05 mm/s were conducted in order to determine the properties of

these aluminium sheets by using an MTS machine. Dimensions of dog-bone samples following the Tensile Testing of Metallic Material Standard (ISO 6892-1:2009) are shown in Fig. 2a. Force and displacement were recorded by the MTS machine, from which the engineering stress-strain curves were calculated. Three tests were conducted on plates with the same thickness. Figure 2b shows the stress-strain curves of plates with 1 mm, 3 mm and 5 mm thickness, respectively. It can be seen that the three test results for each thickness are very close to each other. Therefore, one stress-strain curve for each thickness was selected and plotted in Fig. 2c for comparison. The average mechanical properties of all aluminium sheets are as follow: E (Young's Modulus) = 69 GPa; and σ_Y (Yield stress) = 138 MPa.

2.2.4 *Honeycomb sandwich panel preparation*

The honeycomb sandwich panels were constructed by placing an aluminium honeycomb core in-between two 1 mm thick aluminium plates (face sheets). Prior to adhesive bonding the surface preparation process was carried out according to the ISO 17212 International Standard for surface preparation. In order to provide a rough surface for better bonding with the honeycomb core, the face sheets were sanded at angles of +/- 45 degrees. The plates were then cleaned by using domestic liquid cleaner to remove all dust from the sanding process. Hair dryer was used to dry the plates. Prior to bonding the plates with the core using an adhesive, the plates were once again cleaned using acetone to remove surface oil. A two-component thixotropic epoxy liquid adhesive (FORTIS 825) was used to adhere the face sheets to the core. The mechanical properties of the adhesives are listed in Table 2, as provided by the manufacturer [18].

In order to prevent the adhesives from flowing into the honeycomb structures, one face sheet was bonded to the core first and was left on a flat table with the honeycomb core on top of the

face sheet to dry for 24 hours at room temperature. A weight (bag of sand) was placed on top of the sandwich panels to apply a uniform pressure during the curing period to facilitate the process. Afterwards, another face sheet was bonded to the core by following the same procedure. Finally, 16 equally spaced holes for M10 bolts were drilled through the sandwich panels along their edges.

The honeycomb sandwich panels were grouped as Sandwich Group A, Sandwich Group B, Sandwich Group C, Sandwich Group D and Sandwich Group E, according to the core configurations. Each group consists of five samples, as shown in Table 3.

2.2.5   Monolithic plates

Aluminium alloy 5005 H34 plates with dimension of 300 mm × 300 mm were cut from a 1200 mm × 2400 mm rectangular aluminium plate. The thicknesses of the plates used were 1 mm, 2 mm, 3 mm, 4 mm and 5 mm, respectively. Quasi-static tensile tests for each thickness were carried out to determine the material properties and the results were shown in Fig. 2. Five samples were prepared for each thickness in order to undergo the impact tests. They were labelled as M on Table 4. Then, 16 equally spaced holes for M10 bolts were drilled along the edges on each plate so that the plates could be placed inside the sample holder for the experiment.

2.2.6   Air sandwich panels

The air sandwich panels were constructed using two parallel plates of aluminium alloy 5005 H34 spaced by 16 steel hollow cylinders as spacers, as shown in Fig. 3. Both methods, using the steel hollow cylinders and using a steel frame with the same dimensions as the clamp frame, as the spacer were considered and discussed when constructing the air sandwich panel.

The steel hollow cylinders were chosen because they could allow the air entrapped inside the clamped area to escape quickly to minimize the effect of the entrapped air on the performance of the sandwich panel. Furthermore, due to small magnitude of the impulses, only a small amount localized deformations around the steel cylinders were observed and shown in Fig. 3(c), which did not have significantly effect on the overall deformation of the panel. Only 1 mm plates were used in the construction of the panels. The steel hollow cylinder's outer diameter, height and thickness were 16 mm, 12.7 mm and 1.5 mm respectively.

The height of the steel hollow cylinder was the same as the height of the honeycomb core in order to mimic the sandwich panels without honeycomb core, from which the contribution of honeycomb core could be evaluated. The air sandwich panels were labelled as Sandwich G in Table 3.

3 Test Procedure

The projectiles were fired towards the centre of the samples at five different gas gun pressures: 200 kPa, 500 kPa, 1000 kPa, 1500 kPa and 2000 kPa. Photographs of samples before and after tests were taken and some typical photographs are shown in Fig. 3. The deformation of the projectiles at different impact velocities is shown in Fig. 4. The final deformation of all the back-face sheet and the core were measured using a vernier calliper after cutting the samples along the middle span.

Another group of tests to record the back-face deflection history were conducted at a gun pressure of 1000 kPa; where at this pressure, none of the sandwich panels were fully penetrated by the foam projectile. This was to prevent damaging the laser displacement sensor installed at the back of the sandwich panels. Only one sample each from sandwich

Groups A, B, C, D and monolithic plate of thickness 2 mm and 3 mm was used in these tests. They were labelled as SB-A, SB-B, SB-C, SB-D, SB-M2 and SB-M3 in Table 5, respectively.

4   Results and Discussions

Table 3 and Table 4 summarise the projectile impact velocity, initial momentum, impulse per unit area, measured permanent back-face deflection and failure mode for the aluminium honeycomb sandwich panels, the air sandwich panels and the monolithic plates, respectively. The impulse per unit area generated by the foam projectiles, I_o , is calculated using the formula proposed by Radford et al. [2].

$$I_o = \rho_o l_o v_o \tag{1}$$

where ρ_o is the density of the foam projectile, l_o is the original length of the projectile and v_o is the initial impact velocity of the foam projectile. For the second set of tests, which were to record the deflection history, results for the sandwich panels and the monolithic plates are shown in Table 5.

4.1 Deformation of honeycomb sandwich panels

The deformation of the front-face and the back-face of the honeycomb sandwich panels occurred mainly by stretching and bending while deformation of the core was by progressive buckling. The deformation at the centre of the back-face showed a nose–like shape (Fig. 3b). The whole deformation process can be summarised as follows. Depending on the magnitude of the projectile impulse, the deformation of the front-face progressed up to a maximum before it started to fracture from excessive bending and stretching. Further increasing the impulse promoted the fracture to propagate along the periphery of the projectile on the front-face. At the same time, the core buckled progressively up to full compression. Similar to the

front-face, the back-face was deformed by bending and stretching, which led to full penetration at high impulse level.

Deformation and failure modes of the sandwich panels in the current study are found to be very similar to those observed in the actual blast loading [19]. Therefore, the same argument as presented in [19] will be followed here and the results have been characterised into two groups, i.e., (1) experimental observations and (2) quantitative results.

The experimental observations include the description of the deformation modes and the failure modes of the front-face, the back-face and the honeycomb core. The quantitative results are associated with the impulse applied to the sandwich panels, the permanent back-face deflections and the histories of the back-face deformation captured by the laser displacement sensor.

4.1.1 Experimental observation

Two deformation modes were observed: global deformation and localised deformation. Global deformation is defined as the deformation that reaches the area up to the sandwich clamped edges and it is labelled as Mode G. Localised deformation describes the situation when the deformation area has been limited to the projectiles cross sectional area and when there is no evidence of the plastic hinge line along the clamped edges. Localised deformation has been labelled as Mode L.

The failure mode can be categorised into three types: Type I for indentation, Type F for fracture and Type P for penetration, as shown in Fig. 5. Type I is defined when there is deformation on the face without any fracture. Type F is defined when fracture is present and

starts to propagate. Type P is defined when the projectile penetrates and passes through the face sheets of the sandwich panels. When Type P failure occurs, tensile tearing damage is dominant at the centre while very limited deformation is observed in the remaining part of the sandwich panel. The overall deformation modes and the failure modes for all the sandwich panels are summarised in Fig. 6.

In order to study the deformation of the core, samples A2, B2, C2 and D2, which were tested at similar impulses, were sectioned along the central axis as shown in Fig.7. The core deformation was measured using a vernier calliper and the mean compression strain of the core was calculated accordingly as follows.

$$\varepsilon_c = \frac{\Delta c}{c}$$ (2)

where Δc is the reduction in the core height and c is the initial core height. From the figure, it is evident that the magnitude of the core compression is larger at the centre of the sandwich panels and it decreases towards the edges of the sandwich panels. Due to the difference in the magnitude, the cross section of the sandwich panels may be divided into three regions as shown in Fig. 7. They are: (1) Fully Folding Region, (2) Partly Folding Region, and (3) Folding Absent Region as proposed by Zhu et al. [19].

Similar deformation was also reported in [4, 9, 10, 20]. Almost full compression of the core can be seen in sample A2 which has a core compression ratio of 91%. The core compression ratio of sample B2 and sample C2 were 50% and 79%, respectively. No core compression was observed in sample D2, with only bending of the core. The core used in sample D2 is the densest core with a density of 192.22 kgm^{-3} and the t/l_c ratio of 0.0240.

4.1.2   Quantitative results

The permanent back-face deflections of all the honeycomb sandwich panels against impulses are shown in Fig. 8. Sandwich Group D behaved differently from the other honeycomb sandwich panels as the fitting line shows almost a linear line. The density of the honeycomb core in sandwich Group D is almost 4 times the density of the honeycomb core in sandwich Group A, which is the weakest sandwich group. Linear relations were observed when steel plates were used as the skin and when there was no fracture of the front plate [9-11].

As a very crude estimate, the back-face deformation, δ, is proportional to the applied impact energy e and $e = \frac{1}{2}mv^2$, where m is the mass of the projectile in kg and v is the impact velocity in ms^{-1}. From Eq. (1), $v_o = \frac{I}{\rho_o l_o}$, therefore, $\delta \propto (\frac{m}{2\rho_o^2 l_o^2})I^2$. In order to check the relation between the permanent back-face deflection and impulse, a log-log graph of the deflection is drawn as shown in Fig. 9. The slopes of the graphs vary from 2 to 2.6, which indicate that the back-face deflection and the impulse are related by a power relation. In-depth theoretical analysis is required in order to determine the relationship between the back-face deflection and the applied impulse accurately.

The effects of doubling the foil thickness and increasing the cell size by one and half of the honeycomb core are summarized in Table 6 and Table 7, respectively. Honeycomb Group A and B differs in the foil thickness while honeycomb Group B and C differs in the cell size. Difference in the magnitude of compressive yield stress can be observed from Table 1. Doubling the foil thickness increases the compressive yield stress to almost triple while increasing the cell size by one and a half reduces the compressive yield stress to almost half. Using the weaker core, which is sandwich Group A in Table 6 and Group C in Table 7, as a reference for the comparison, the percentage reduction of the back-face are calculated at similar impulse. The data demonstrates that the percentage reduction of the back-face is

significant at low impulse. The average percentage reduction of the back-face deflection is 55% when doubling the foil thickness and is 36% when the cell size is reduced from 4.763 mm to 3.175 mm.

4.2 Deflection history of honeycomb sandwich panels and monolithic plates

Figure 10 shows the typical back-face deflection history for samples SB-A, SB-B, SB-C, SB-D, SB-M2 and SB-M3. From the Figure, the elastic spring-back which is defined as the difference between the maximum deflection and the permanent deflection of the back-face, is measured. The elastic spring-back for the sample SB-A, SB-B, SB-C, SB-D, SB-M2 and SB-M3 are 2 mm, 4 mm, 2 mm and 3.5 mm, 2.5 mm and 3 mm respectively as shown in Table 5. The largest spring-back is 4 mm attained by sample SB-B and 3 mm attained by monolithic plate SB-M3. The result illustrates that honeycomb sandwich panels do not have a significant influence on the elastic spring-back effect compared with monolithic plates at the impulse level studied.

4.3 Comparison between honeycomb sandwich panels, air sandwich panels and monolithic plates

Six samples of air sandwich panels (sandwich Group G) were tested and the results are listed in Table 3. Photographs of the air sandwich panels before and after the tests are shown in Fig. 3c. The impact velocities were varied from 103 m/s to 365 m/s. The permanent back-face deflection of the air sandwich panels were compared with that of sandwich Groups A, B and C (representing sandwich panel structure). The comparison can be seen in Fig. 11. Sandwich Groups D and E were omitted in the figure for clarity.

Each group was represented by the best fitted line. However, limited data for each group (4 points) was due to the following two reasons:

1. Large size of samples (300 mm×300 mm) and limited stock of honeycomb cores;

2. The maximum impulse that can be generated by the current testing equipment. The gas gun employed in this study (barrel length of 3 m and diameter of 38 mm) has a maximum operational pressure of 2 MPa. This maximum pressure could speed up the foam projectile up to 370 m/s. At this impact velocity, the impulse per unit area was around 5.5 $kNsm^{-2}$.

The differences can be summarised by dividing the graph into three different regions according to the intersection of sandwich Group G with sandwich Group A (the weakest sandwich group) and with sandwich Group B (the strongest sandwich group in the comparison) as shown in Fig. 11. The regions are classified as low impulse region, medium impulse region and high impulse region. The low impulse region covers from 0 to 2.3 $kNsm^{-2}$. In this region, the air sandwich panels perform better than the honeycomb sandwich panels in minimising the back-face deflection. The front-face sheet of the air sandwich panels has ample time and space to deform before it reaches the back-face sheet. Mode G deformation is observed at the front-face sheets of the air sandwich panels which indicates more energy being absorbed by the front-face sheets. As a comparison, the front-face sheets of the honeycomb sandwich panels show Mode L deformation. For sample G1, the front-face sheet of the air sandwich panel deforms individually even at an impulse level of 1.57 $kNsm^{-2}$, and therefore there is no back-face deformation.

When the deformation of the front-face sheet of an air sandwich panel reaches 12.7 mm, the remainder of the impact energy is then transferred to the back-face sheet and this deforms it.

The contact area between the front-face sheet and the back-face sheet is larger due to Mode G deformation of the front-face sheet. This phenomenon further reduces the stress concentration on the back-face sheet thus reducing the deflection.

The advantage of the air sandwich panels against the honeycomb sandwich panels ceases when the impulse reaches 2.3 $kNsm^{-2}$. This is the beginning of the medium impulse region which covers up to 4.70 $kNsm^{-2}$. At an impulse level of 2.3 $kNsm^{-2}$, sandwich Group A, which is the weakest sandwich group, starts to deform less than the air sandwich panels. In this region, the progressive buckling of the honeycomb core absorbs a large amount of impact energy and reduces the back-face deflection.

The third region is the high impulse region which covers an impulse level from 4.70 $kNsm^{-2}$ and beyond. In this region the air sandwich panels again outperformed the honeycomb sandwich panels. Fracture of the front-face sheets are observed in all honeycomb sandwich panels in this region. It is believed that the fracture has weakened the sandwich panels. According to the test result conducted on monolithic plates M1-4 in Table 4, the aluminium face sheet of 1 mm thick can deform up to 32 mm before fracture. The stress concentration that developed at the interface between the front-face sheet and the core edges has weakened the face sheet and limited the face sheet to deform more before fracture. Also according to the result of testing monolithic plates M1-4, the air sandwich panels can be further optimised by increasing the gap between the two plates to 32 mm.

Figure 11 also shows the comparison between the air sandwich panels and the monolithic plates of thickness 2 mm at increasing impulses. This comparison indicates that the air

sandwich panels outperform the monolithic plates of equivalent mass at all impulse regions applied in this study.

A similar observation was reported by Roach at el. [21] where it was concluded that the panel specially designed to absorb energy might best be constructed from a series of thin laminates with air spaces, rather than from single thick laminates or a laminate with core. The distance between the laminates should be sufficient to allow for plate deflection during the deformation process. However, the ballistic limit, which was defined as the velocity just enough to have a penetration, of sandwich panels was higher compared to parallel plate without core as observed by Hou at el. [22]. Note that projectiles made of solid materials, rather than aluminium foam, were used in both [20] and [21].

4.4 Comparison between honeycomb sandwich panels with monolithic plates

The back-face deflections of the honeycomb sandwich panels have been compared with the deflection of the monolithic plates with equivalent mass. The deflections of the plates at various impulse levels were recorded and shown in Table 4 (samples M1-1 to M4-4). At least 4 different impulses were loaded to the plates with the same thickness. In order for the monolithic plates to have the same equivalent mass as the honeycomb sandwich panels, the monolithic plates need to have a thickness of 2.55 mm, 2.84 mm, 2.71 mm, 3.36 mm and 2.80 mm for sandwich groups A, B, C, D and E respectively, which was impossible practically. Hence the data for the required plate thickness have been generated using interpolation in-between the experimental results, as shown in Fig. 12.

The permanent back-face deflection of the honeycomb sandwich panels and the monolithic plates have been compared in Fig. 13. In this figure, only sandwich Group A, Group B and

Group C are used for the comparison with the monolithic plates with equivalent mass. Sandwich Group E has been omitted because panels' properties are almost similar to the properties of sandwich Group A. Sandwich panels in group D are relatively strong and the experimental data points do not representing the general behaviour of the sandwich panels. The sandwich panels should be loaded with projectile at higher impact velocity however; this test is unable to be carried out due to equipment limitation. Therefore, due to the insufficient data point especially at higher impulse to describe the deformation, sandwich Group D has also been omitted from the comparison.

From Fig. 13, the honeycomb sandwich panels outperform their monolithic plates of equivalent mass up to a critical impulse. Beyond this critical impulse, the honeycomb sandwich panels deform more. The critical impulse for sandwich Groups A, B and C are 4.3 kNsm^{-2}, 4.8 kNsm^{-2} and 4.6 kNsm^{-2} respectively. Similar observations have also been reported [11] and it was concluded that the accumulated plastic strains that develop in the front-face of the sandwich panels exceed those in the monolithic plate at relatively high impulse.

5 Conclusions

Honeycombs sandwich panels with 1 mm thick aluminium face sheets and five different honeycomb core configurations have been impacted with aluminium foam projectiles at various speeds. The back-face deflection of the honeycomb sandwich panels has been recorded and compared to determine the effect of the core configurations. It has been found that the foil thickness and the cell size of the core affect the back-face deflection of the honeycomb sandwich panels. Increasing the foil thickness and reducing the cell size led to a decrease in the back-face deflection, but increases the overall honeycomb sandwich panels'

weight. Optimization between impact resistance and weight of a honeycomb sandwich panel design is one of the important issues that need to be considered in future.

The use of honeycomb sandwich panels in absorbing the impact energy of aluminium foam projectiles is limited by the operational impulse range. The operational impulse range has to be determined to ensure the effectiveness of the sandwich panels as a protective structure. Beyond the operational range, replacement of honeycomb sandwich panels with air sandwich panels or monolithic plates of equivalent mass can be more favourable.

It was found that a honeycomb sandwich panel has to deform as an integral structure (face sheets and honeycomb core deform together) in order to effectively absorb impact energy and minimise the back-face deflection. Selection of components in constructing a sandwich panel is important in order to ensure the optimum performance of the panel. The core must allow the front-face to deform to its maximum before fracture. Once the front-face fractures, the overall impact resistance of the sandwich panels reduces significantly.

Acknowledgements

References

[1] G. Lu, T.X. Yu, Energy Absorption of Structures and Materials, CRC Press, 2003.

[2] D.D. Radford, V.S. Deshpande, N.A. Fleck, The use of metal foam projectiles to simulate shock loading on a structure, Int. J. Impact Eng. 31 (2005) 1152-1171.

[3] D.D. Radford, N.A. Fleck, V.S. Deshpande, The response of clamped sandwich beams subjected to shock loading, Int. J. Impact Eng. 32 (2006) 968-987.

[4] H.J. Rathbun, D.D. Radford, Z. Xue, M.Y. He, J. Yang, V.S. Deshpande, N.A. Fleck, J.W. Hutchinson, F.W. Zok, A.G. Evans, Performance of metallic honeycomb-core sandwich beams under shock loading, Int. J. Solids Struct. 43 (2006) 1746-1763.

[5] V.L. Tagarielli, V.S. Deshpande, N.A. Fleck, The dynamic response of composite sandwich beams to transverse impact, Int. J. Solids Struct. 44 (2007) 2442-2457.

[6] V. Rubino, V.S. Deshpande, N.A. Fleck, The dynamic response of end-clamped sandwich beams with a Y-frame or corrugated core, Int. J. Impact Eng. 35 (2008) 829-844.

[7] V.L. Tagarielli, V.S. Deshpande, N.A. Fleck, Prediction of the dynamic response of composite sandwich beams under shock loading, Int. J. Impact Eng. 37 (2010) 854-864.

[8] B.P. Russell, T. Liu, N.A. Fleck, V.S. Deshpande, The soft impact of composite sandwich beams with a square-honeycomb core, Int. J. Impact Eng. 48 (2012) 65-81.

[9] D.D. Radford, G.J. McShane, V.S. Deshpande, N.A. Fleck, The response of clamped sandwich plates with metallic foam cores to simulated blast loading, Int. J. Solids Struct. 43 (2006) 2243-2259.

[10] G.J. McShane, D.D. Radford, V.S. Deshpande, N.A. Fleck, The response of clamped sandwich plates with lattice cores subjected to shock loading, Eur. J. Mech. A-Solids 25 (2006) 215-229.

[11] V. Rubino, V.S. Deshpande, N.A. Fleck, The dynamic response of clamped rectangular Y-frame and corrugated core sandwich plates, Eur. J. Mech. A-Solids 28 (2009) 14-24.

[12] J.Shen, G. Lu, Z.H. Wang and L.M. Zhao, Experiments on curved sandwich panels under blast loading. Int. J. Impact Eng. 37 (2010) 960-970.

[13] S.M. Pingle, N.A. Fleck, H.N.G. Wadley, V.S. Deshpande, Discrete element calculations of the impact of a sand column against rigid structures, Int. J. Impact Eng. 45 (2012) 74-89.

[14] Columbia Accident Investigation Board, Report Volume 1, NASA, 2003.

[15] J.D. Walker, From Columbia to Discovery: Understanding the impact threat to the space shuttle, Int. J. Impact Eng. 36 (2009) 303-317.

[16] A. Neuberger, S. Peles, D. Rittel, Springback of circular clamped armor steel plates subjected to spherical air-blast loading, Int. J. Impact Eng. 36 (2009) 53-60.

[17] E.W. Andrews, G. Gioux, P. Onck, L.J. Gibson, Size effects in ductile cellular solids. Part II: Experimental results, Int. J. Mech. Sci. 43 (2001) 701-713.

[18] FORTIS AD825 Product Data, http://fortisadhesives.com/adhesives.php, viewed on 1st April 2014.

[19] F. Zhu, L. Zhao, G. Lu, Z. Wang, Deformation and failure of blast-loaded metallic sandwich panels—Experimental investigations, Int. J. Impact Eng. 35 (2008) 937-951.

[20] M.T. Tilbrook, D.D. Radford, V.S. Deshpande, N.A. Fleck, Dynamic crushing of sandwich panels with prismatic lattice cores, Int. J. Solids Struct. 44 (2007) 6101-6123.

[21] A.M. Roach, K.E. Evans, N. Jones, The penetration energy of sandwich panel elements under static and dynamic loading. Part I, Compos. Struct. 42 (1998) 119-134.

[22] W. Hou, F. Zhu, G. Lu, D.N. Fang, Ballistic impact experiments of metallic sandwich panels with aluminium foam core, Int. J. Impact Eng. 37 (2010) 1045-1055.

Captions of figures

Fig. 1. Impact experimental set-up.

Fig. 2. Quasi-static testing of aluminium alloy 5005 H34: (a) sketch of sample dimensions; (b) stress-strain curves obtained from three repeated tests of samples with 1 mm, 3 mm and 5 mm thickness respectively; (c) typical stress- strain curves of samples with 1 mm, 2 mm, 3 mm, 4 mm and 5 mm thickness.

Fig. 3. Photographs showing typical deformation of (a) a monolithic plate (sample M1-2); (b) a honeycomb sandwich panel (sample B4); (c) an air sandwich panel (sample G6).

Fig. 4. Photographs of aluminium foam projectiles: (a) initial shape; (b) and (c) after tests at 189.39 m/s and 333.33 m/s impact velocities, respectively.

Fig. 5. Typical failure modes of the front-face of honeycomb sandwich panels: (a) Type P (penetration) (b) Type F (fracture); (c) Type I (indentation)

Fig. 6. Deformation modes and failure modes of honeycomb sandwich panels with different core configurations.

Fig. 7. Four specimens showing core compression ratio reduces from the centre towards the edges of the sandwich panels. From top to bottom: samples A2, B2, C2 and D2.

Fig. 8. Permanent back-face deflection of honeycomb sandwich panels at various impulse levels.

Fig. 9. The log-log graph of the permanent back-face deflection of honeycomb sandwich panels *vs*. impulse.

Fig. 10. Typical back-face deflection histories of honeycomb sandwich panels and monolithic plates.

Fig. 11. Permanent back-face deflection of the honeycomb sandwich panels (Groups A, B and C) , the air sandwich panels (Group G) and 2 mm monolithic plates.

Fig. 12. Permanent deflection of the monolithic plates.

Fig. 13. Critical impulse of honeycomb sandwich panels Groups A, B and C.

Table 1. Properties of aluminium honeycombs in the out-of-plane direction (data were provided by the manufacturer)

Group	Designation	Density ρ (kg/m^3)	Cell Size l_c (mm)	Foil Thickness t (mm)	Comp. Yield Stress (MPa)	Modulus (GPa)	$\dfrac{t}{l_c}$
A	3.1-1/8-.0007	49.66	3.18	0.018	2.07	0.52	0.006
B	6.1-1/8-.0015	97.71	3.18	0.038	7.03	1.66	0.012
C	4.4-3/16-.0015	70.48	4.76	0.038	3.78	1.00	0.008
D	12-1/8-.0030	192.22	3.18	0.076	19.96	6.21	0.024
E	3.4-1/4-.0015	54.46	6.35	0.038	2.55	0.62	0.006

Table 2. Properties of epoxy adhesive AD825 [13]

Elastic Modulus in Compression (GPa)	Compressive Strength (MPa)	Tensile Bond Strength (Al/AI at 25°C) (MPa)	Flexural Strength (MPa)	Tensile Strength (MPa)
1.99	85-90	12	30	35

Table 3. Summary of experimental results: honeycomb sandwich panels

Sample	Honeycomb Cell Size (mm)	Honeycomb Foil Thickness (mm)	Impact Velocity (m/s)	Initial Momentum (kgm/s)	Impulse I (kNsm^{-2})	Back Face Deflection (mm)	Type of Failure Front Face	Type of Failure Core	Type of Failure Back Face
A1	3.18	0.018	106.38	1.68	1.55	3	I	I	I
A2	3.18	0.018	200.00	3.26	3.04	7	I	I	I
A3	3.18	0.018	289.02	4.68	4.37	18	F	I	I
A4	3.18	0.018	320.51	5.54	5.18	36	P	F	I
A5	3.18	0.018	359.71	6.04	5.58	P	P	P	P
B1	3.18	0.038	109.17	1.71	1.54	1	I	I	I
B2	3.18	0.038	189.39	3.03	2.81	4	I	I	I
B3	3.18	0.038	292.40	4.50	4.20	8	I	I	I
B4	3.18	0.038	357.14	5.64	5.24	27	P	I	I
B5	3.18	0.038	354.61	5.35	5.13	26	P	I	I
C1	12.70	0.038	111.11	1.77	1.62	2	I	I	I
C2	12.70	0.038	203.25	3.15	2.94	5	I	I	I
C3	12.70	0.038	285.71	4.71	4.39	13	F	I	I
C4	12.70	0.038	324.68	5.06	4.74	22	P	P	F
C5	12.70	0.038	367.65	6.23	5.32	P	P	P	P
D1	3.18	0.076	110.62	1.68	1.62	0	No deformation		
D2	3.18	0.076	198.41	3.35	3.12	6	I	I	I
D3	3.18	0.076	280.90	4.75	4.45	15	I	I	I
D4	3.18	0.076	333.33	5.87	5.51	17	F	I	I
D5	3.18	0.076	352.11	6.23	5.49	20	F	I	I
E1	6.35	0.038	154.32	2.25	2.14	3	I	I	I
E2	6.35	0.038	228.31	3.40	3.25	5	I	I	I
E3	6.35	0.038	314.47	4.47	4.31	14	F	F	I
E4	6.35	0.038	349.65	5.10	4.90	28	P	P	F
E5	6.35	0.038	375.94	5.38	5.23	P	P	P	P
G1			103.31	1.64	1.57	0	I		/
G2			200.00	3.22	3.01	7	I		I
G3			310.56	5.03	4.83	16	I		I
G4			352.11	5.42	5.24	19	I		I
G5			354.61	5.67	5.41	24	P		F
G6			364.96	5.84	5.55	P	P		P

Note: I: Indentation, F: Fracture, P: Penetration.

Table 4. Summary of experimental results: monolithic plates

Sample	Thickness (mm)	Impact Velocity (m/s)	Initial Momentum (kgm/s)	Impulse I (kNsm^{-2})	Back Face Deflection (mm)	Type of failure
M1-1	1	113.64	1.73	1.58	13	I
M1-2	1	183.82	2.78	2.59	23	I
M1-3	1	220.26	3.33	3.09	29	I
M1-4	1	255.10	3.80	3.56	32	I
M1-5	1	297.62	4.26	3.95	/	P
M2-1	2	216.45	2.71	2.54	12	I
M2-2	2	333.33	4.37	4.12	18	I
M2-3	2	333.33	4.47	4.17	21	I
M2-4	2	370.37	5.15	4.82	25	I
M3-1	3	207.47	2.74	2.47	7	I
M3-2	3	331.13	4.27	4.08	13	I
M3-3	3	333.33	4.57	4.29	15	I
M3-4	3	362.32	5.22	4.96	18	I
M4-1	4	222.22	2.91	2.76	0	/
M4-2	4	331.13	4.27	3.92	7	I
M4-3	4	337.84	4.53	4.25	9	I
M4-4	4	373.13	5.30	4.96	12	I

Note: I: Indentation, F: Fracture, P: Penetration.

Table 5. Summary of experimental results: the spring-back effect of honeycomb sandwich panels and monolithic plates

Sample	Gas Gun Pressure (kPa)	Impulse I (kNsm^{-2})	Maximum Deflection (mm)	Final Deflection (mm)	Spring back (mm)
SB-A	1000	3.77	15.0	13.5	1.5
SB-B	1000	3.82	14.0	10.0	4.0
SB-C	1000	3.89	14.0	12.0	2.0
SB-D	1000	3.77	6.5	3.0	3.5
SB-M2	1000	3.81	22.5	20.0	2.5
SB-M3	1000	3.66	19.0	16.0	3.0

Table 6. The comparison between sandwich panels Group A and sandwich panels Group B (The aluminium honeycomb core in sandwich panels Group B has the same cell size, but double foil thickness as that in sandwich panels Group A.)

Pressure	Ave. Impulse	Deflection		Back-face deflection reduction
		Sandwich A	Sandwich B	
(kPa)	(kNsm^{-2})	(mm)	(mm)	(%)
200	1.55	3	1	67
500	2.93	7	4	43
1000	4.29	18	8	56

Table 7. The comparison between sandwich panels Group B and sandwich panels Group C (The aluminium honeycomb core in sandwich panels Group C has the same foil thickness, but larger cell size as that in sandwich panels Group B.)

Pressure	Ave. Impulse	Deflection		Back face deflection reduction
		Sandwich B	Sandwich C	
(kPa)	(kNsm^{-2})	(mm)	(mm)	(%)
200	1.58	1	2	50
500	2.88	4	5	20
1000	4.29	8	13	38

Pressure Regulator

Gas Chamber

Barrel of Gas Gun

Velocity Meter

Sample Holder

Laser Displacement Sensor

I-Beam

Nitrogen Gas Tank

Front View of Sample Holder

(a)
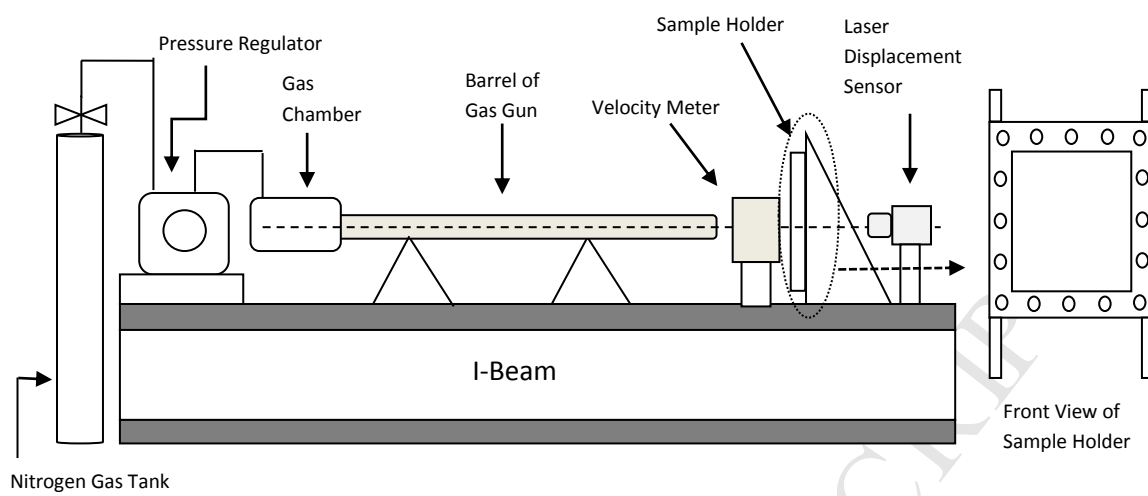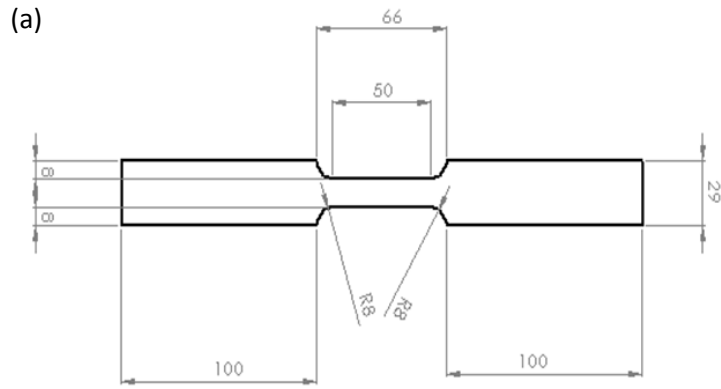
(Dimensions are in mm)

(b)

(c)
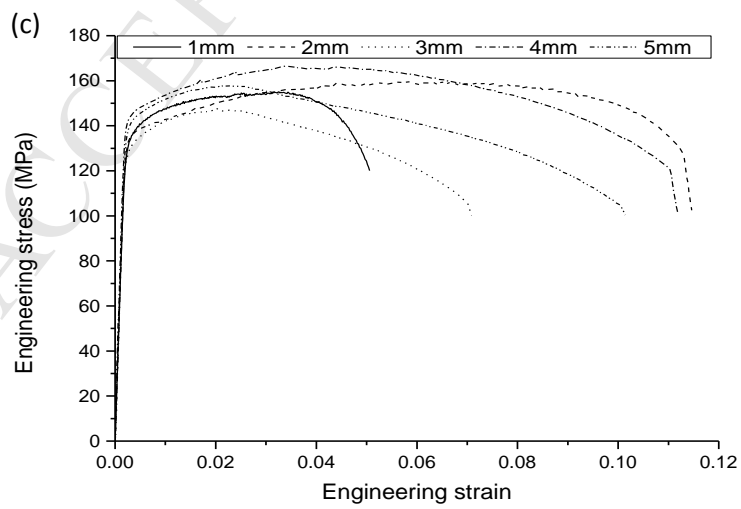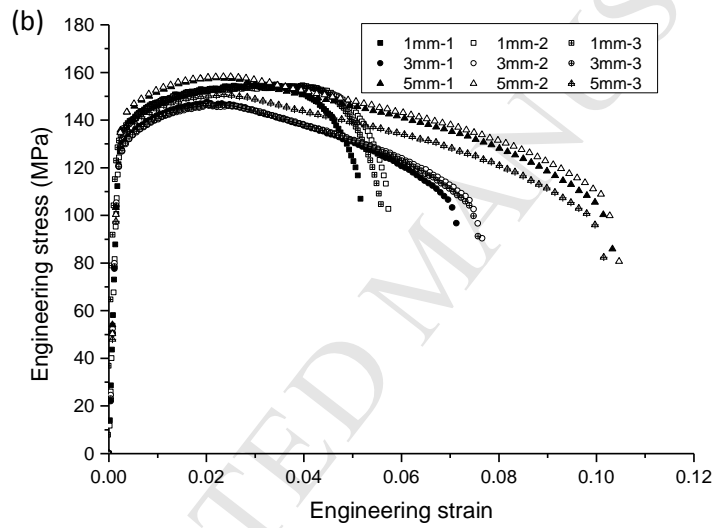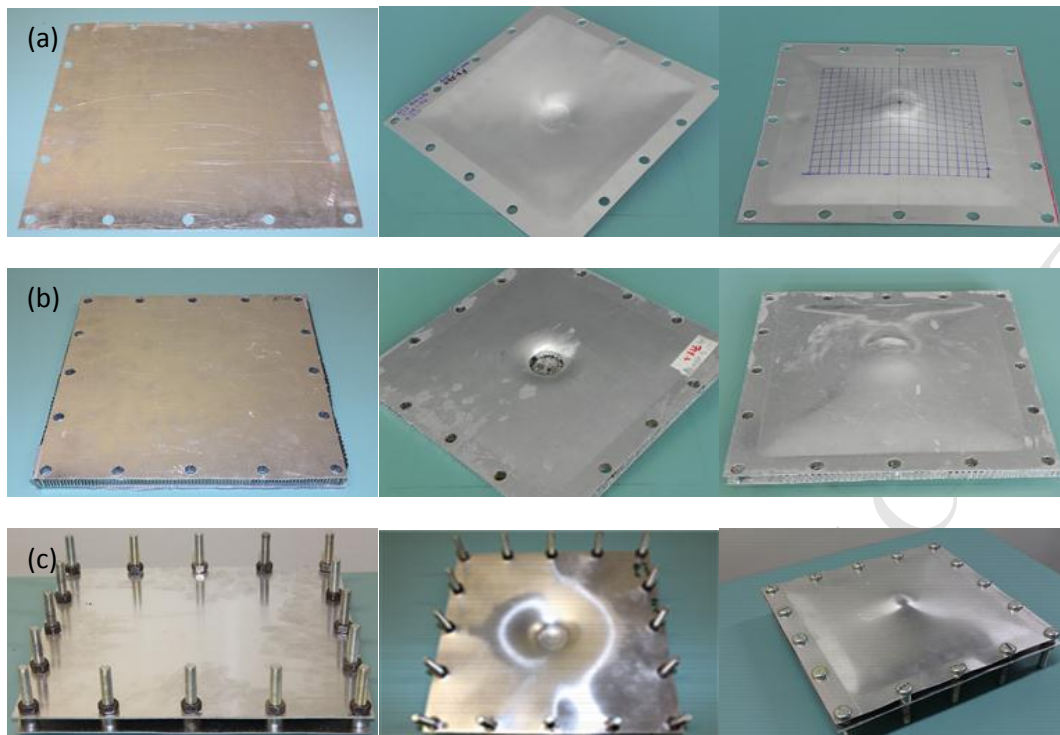
| | Initial shape | After tests: front-face | After tests: back-face |

(a)   (b)   (c)

(a)   (b)   (c)

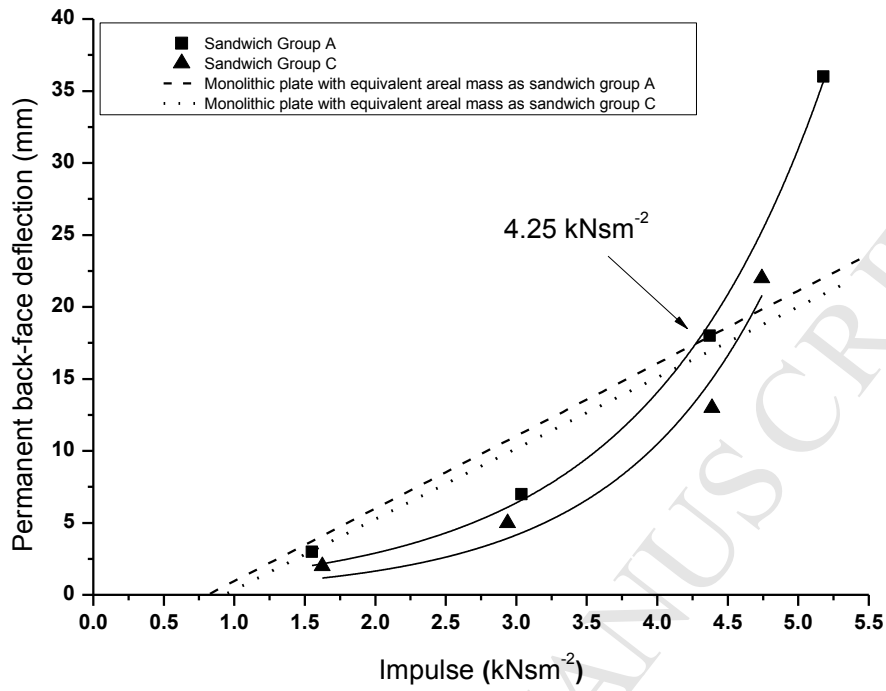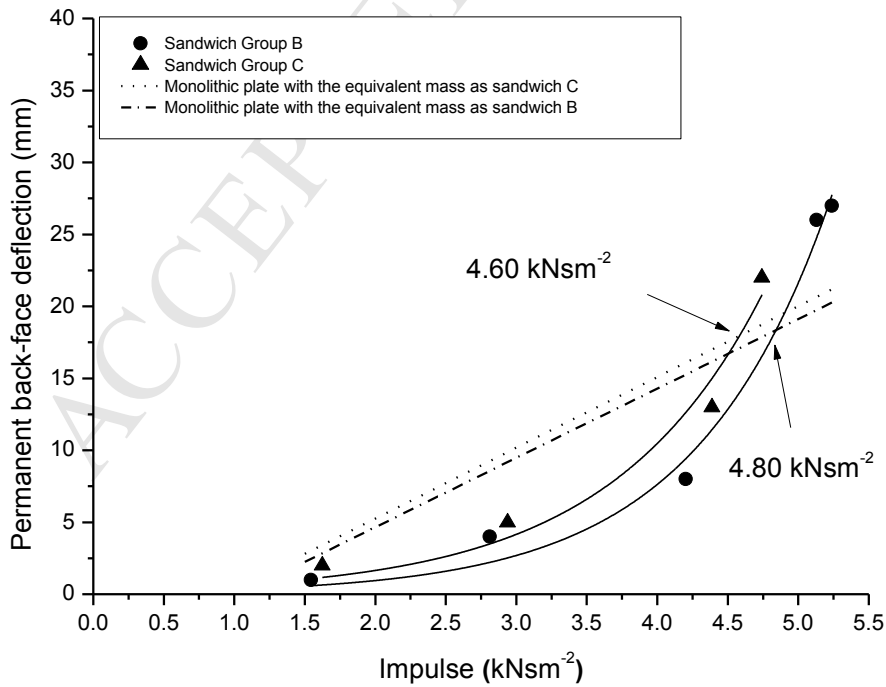Fully Folding Region   Partly Folding Region   Folding Absent Region
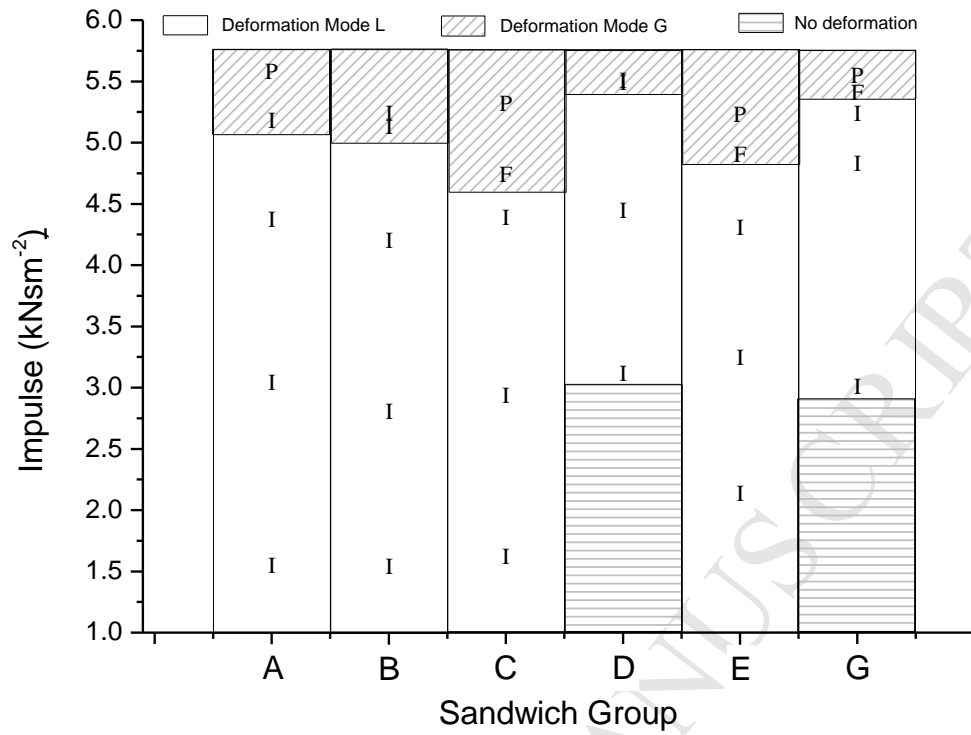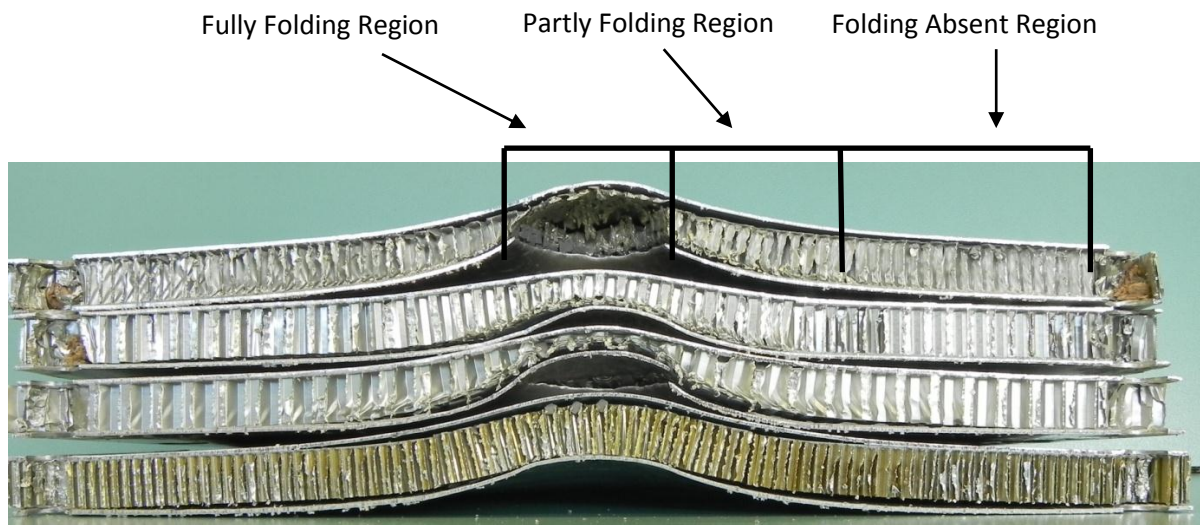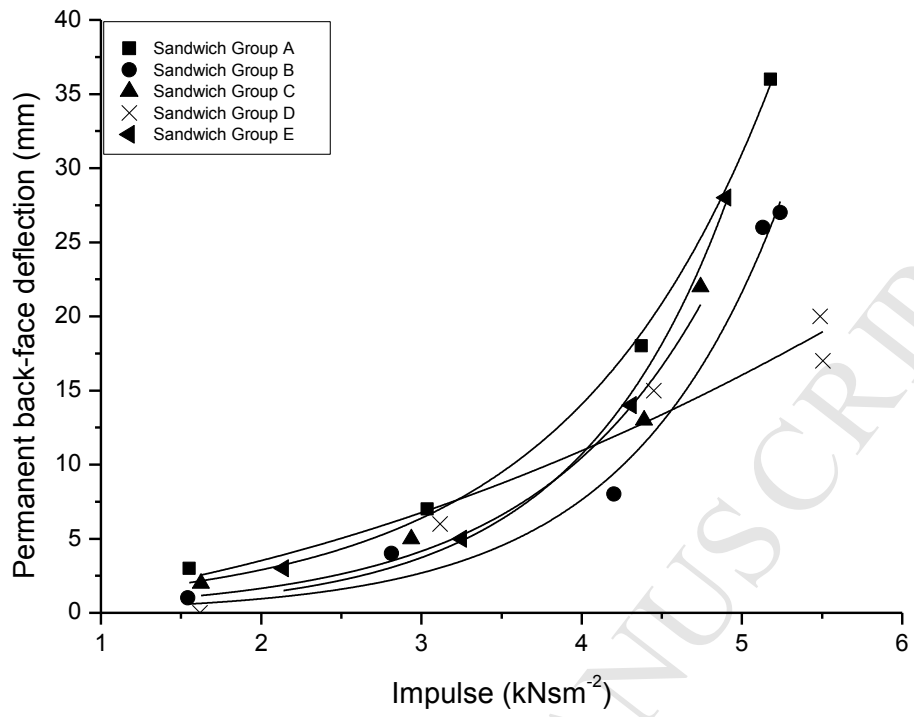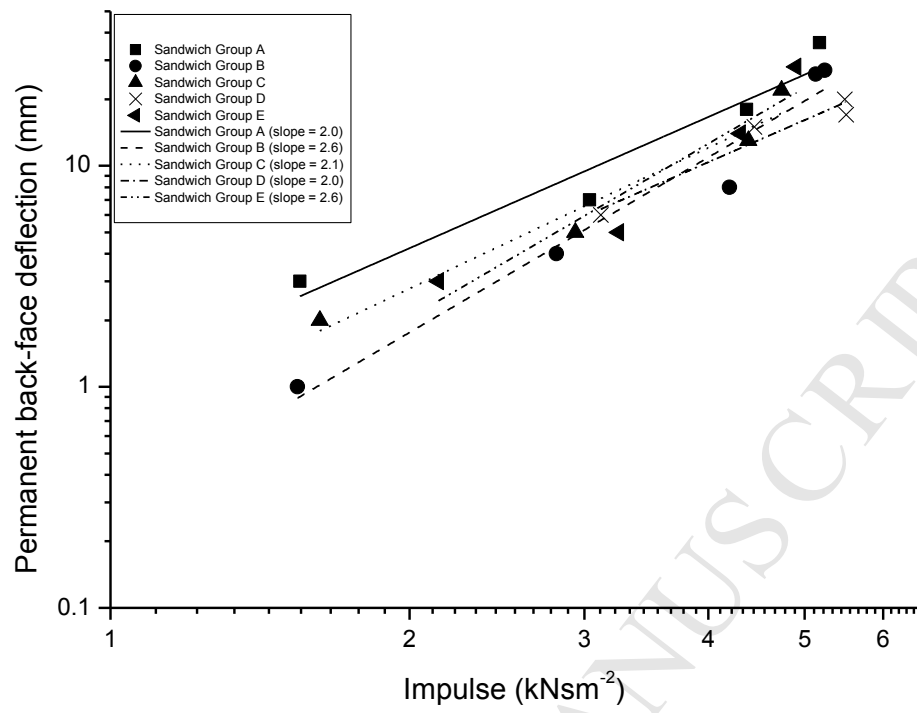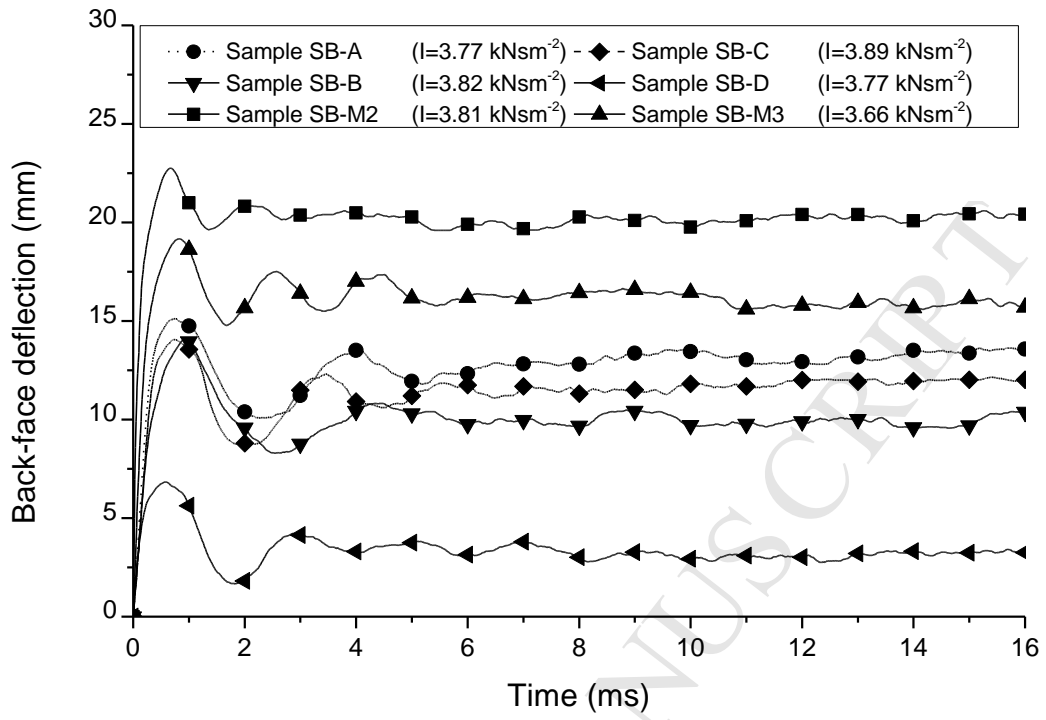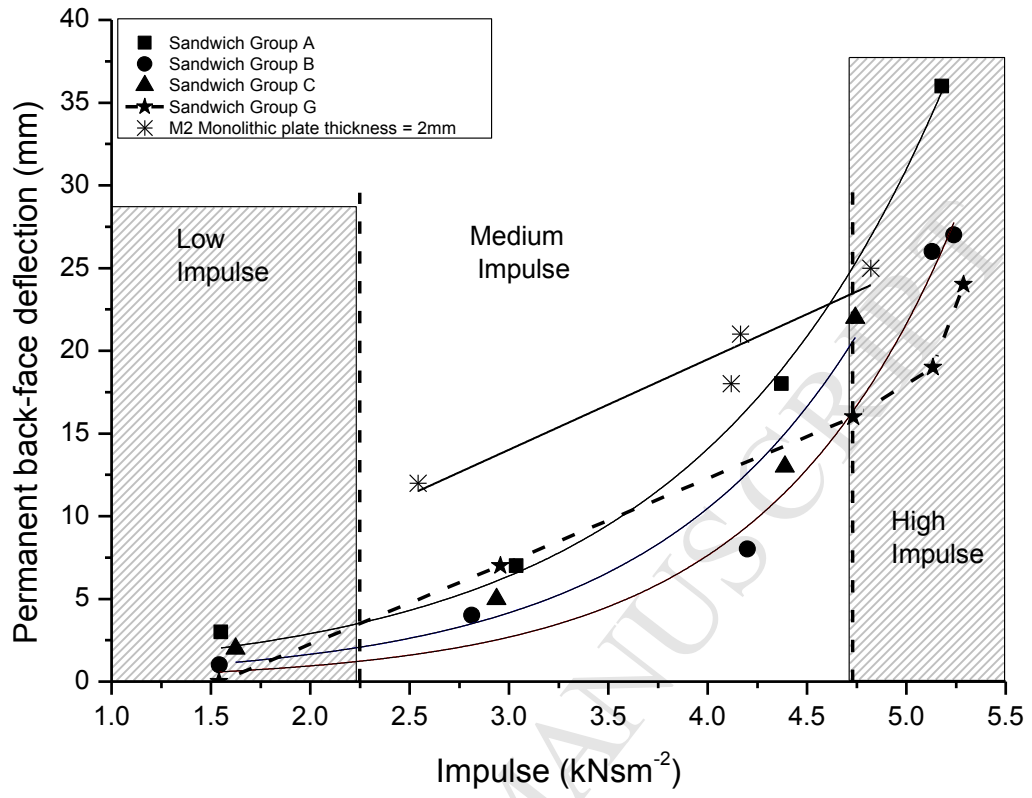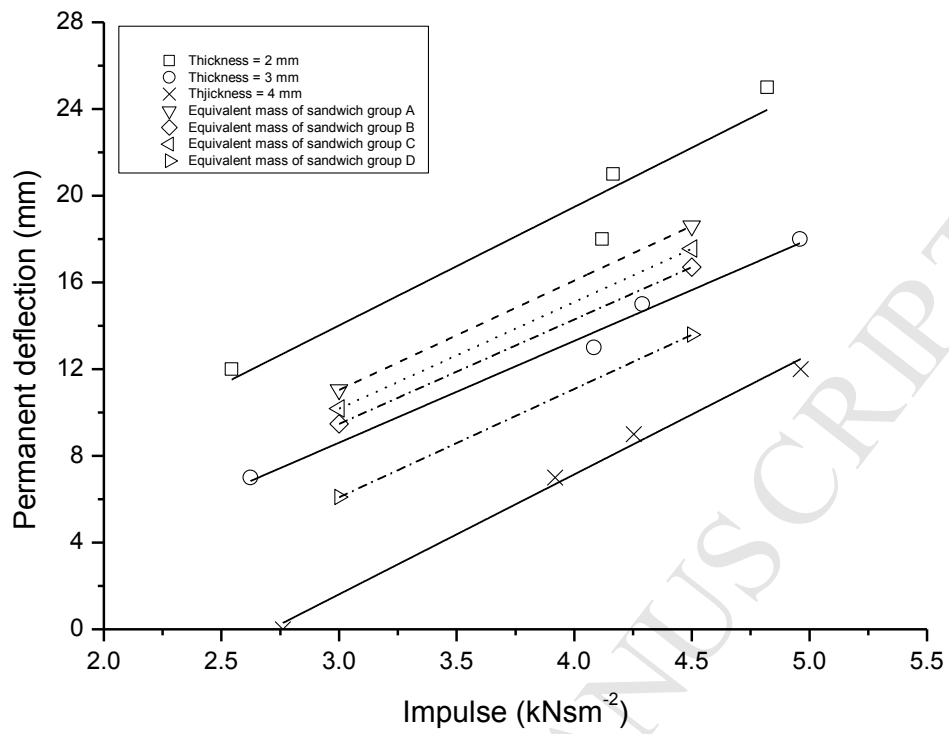
(a)

(b)

Highlights

- The effects of core properties towards minimising the back-face deflection of honeycomb core sandwich panels upon impact by foam projectiles were studied.

- The back-face deflections of the sandwich panels were also compared with monolithic plate of equivalent mass and air sandwich panels.

- Histories of the back-face deflections were also recorded using a laser displacement sensor.

- Advantages and limitations of sandwich panels compared with monolithic plates of equivalent mass and air sandwich panels were discussed.